

DOI [10.24425/ae.2021.137582](https://doi.org/10.24425/ae.2021.137582)

# Influence of road excitation on thermal field characteristics of the water-cooled IWM

JIE FENG, DI TAN\*, MENG YUAN

Shandong University of Technology, School of Transportation and Vehicle Engineering  
266 Xincun West Road, Zhangdian District, Shandong Province, Zibo, China

\*e-mail: [tandi@sdut.edu.cn](mailto:tandi@sdut.edu.cn)

(Received: 12.01.2021, revised: 17.03.2021)

**Abstract:** The in-wheel motor is installed in wheels, and road excitation acts on the in-wheel motor directly through a wheel, which affects the flow field characteristics of the motor's liquid cooling system, and affects the thermal field characteristics of the in-wheel motor. Aiming at this problem, the in-wheel motor drive system is taken as the research object in this paper. Firstly, the heat flow coupling analysis model of the in-wheel motor drive system is established by using the heat flow coupling theory. Then the vibration response of in-wheel motor stator and shell under different road excitation obtained from the previous study is taken as the load. Finally, thermal field characteristics of the water-cooled the in-wheel motor under different working conditions are studied, and the influence law of different speed and road grades on the thermal field characteristics is obtained. The results show that under the road excitation, the maximum temperature of each component of the in-wheel motor decreases due to the vibration effect of road excitation on the flow field of the cooling system, and the decrease of the stator and winding is the most obvious. Additionally, the higher the speed, the greater the road roughness coefficient, the greater the temperature drop of each component of the in-wheel motor. However, the thermal field distribution of local parts of the motor is relatively uneven under road excitation, which leads to greater thermal stress of the local parts and increases the risk of motor damage.

**Key words:** in-wheel motor drive system, road excitation, thermal field characteristics, water-cooled in-wheel motor

## 1. Introduction

The in-wheel motor (IWM) is installed in wheels; it needs to meet the requirements of high power density and high-torque density. At the same time, because the installation space is narrow



© 2021. The Author(s). This is an open-access article distributed under the terms of the Creative Commons Attribution-NonCommercial-NoDerivatives License (CC BY-NC-ND 4.0, <https://creativecommons.org/licenses/by-nc-nd/4.0/>), which permits use, distribution, and reproduction in any medium, provided that the Article is properly cited, the use is non-commercial, and no modifications or adaptations are made.

and closed, the air flow is not smooth, which makes the heat dissipation capacity of the IWM poor. If the heat of the IWM cannot be dissipated in time, it will threaten the safety and stability of the IWM drive system and vehicle [1–4]. Therefore, the accurate study of the thermal field characteristics of the IWM drive system under different road excitation is of great importance to the structural optimization of the subsequent IWM cooling system and to ensure the safe operation of the IWM.

The thermal field characteristics of the water-cooled IWM have been studied by scholars at home and abroad. In reference [5], the water-cooled IWM was taken as the research object, and the temperature characteristics of the IWM under rated and peak operating conditions were calculated and analyzed. Based on the influence of the thermal characteristics of the external rotor IWM in the vehicle's external flow field, the thermal fields of each part of the water-cooled IWM under natural air cooling and oil cooling were compared and analyzed in reference [6]. In reference [7], the thermal field of the water-cooled IWM under normal driving, off-road driving and uphill driving conditions was simulated and analyzed, and the maximum inlet water temperature of the IWM was obtained under the above three conditions. In reference [8, 9], the three dimensional flow field and thermal field of the water-cooled permanent magnet synchronous motor were calculated and analyzed under rated conditions. In reference [10], the electromagnetic-heat-fluid coupling analysis model of the water-cooled IWM was established, and the thermal analysis of the water-cooled IWM under rated working conditions was carried out, and the distribution positions of the highest and lowest temperatures of the motor were obtained. In reference [11, 12], the thermal field of the water-cooled IWM under rated load was analyzed.

In conclusion, the research on the thermal field characteristics of the water-cooled IWM at home and abroad is mostly carried out under the ideal assumptions, that is, road excitation is not considered. In fact, the IWM is installed in wheels, and road excitation will act on the IWM directly through the wheel, which will affect the flow field characteristics of the motor's liquid cooling system, and then affect the thermal field characteristics of the IWM. Therefore, the accurate analysis of the thermal field characteristics of the water-cooled IWM under different road excitation plays a crucial role in the accuracy of the research on heat dissipation of the IWM.

Based on the above, the IWM drive system is taken as the research object based on the heat flux coupling analysis model of the IWM drive system in this paper. And the time-domain response of vibration velocity of the stator and shell of the water-cooled IWM under different road excitation obtained from the previous study is taken as the load to systematically analyze the thermal field characteristics of the IWM drive system. The influence law of different speed and road grade on its thermal field characteristics is obtained, which lays a certain foundation for the subsequent cooling structure optimization of the IWM.

## 2. Research method

The interaction of a vibration field, electromagnetic field, flow field, thermal field and other physical fields is involved in the study of thermal field characteristics of the water-cooled IWM under road excitation. To solve this problem, the research methods shown in Fig. 1, below, are adopted in this paper.

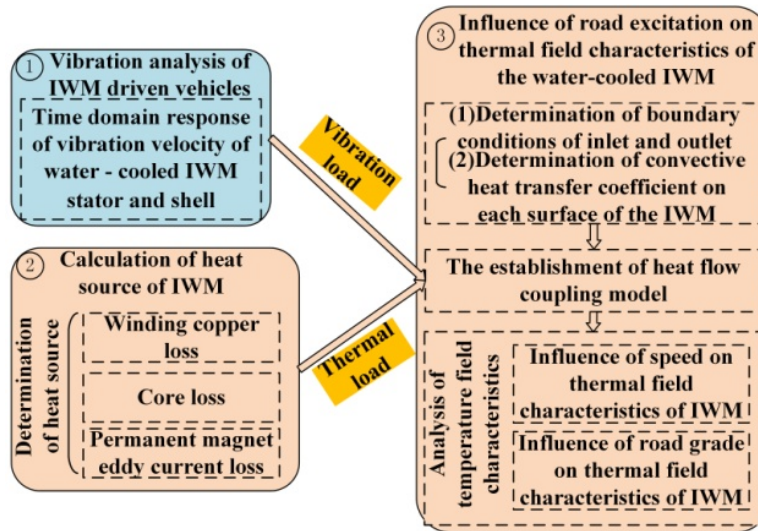


Fig. 1. Research method

As shown in Fig. 1, the study of thermal field characteristics of the water-cooled IWM under road excitation in this paper is divided into three steps. The first step is the vibration analysis of the IWM driven vehicle. Through the vibration analysis of the IWM driven vehicle, the response characteristics of the stator and shell vibration velocity of the IWM driven system under different speeds and road grades are obtained. This part of work has been completed in reference [13]. The second step is the calculation of a heat source for the water-cooled IWM. The heat source of the motor is composed of the loss of the motor winding, the loss of the fixed rotor core and the eddy current loss of the permanent magnet. The loss of each component is calculated by a formula, and the heat rate is converted by a heat source formula, so as to obtain the thermal load of each component. The third step is the analysis of thermal field characteristics of the water-cooled IWM under road excitation. Firstly, the heat flow coupling model is established by applying the heat flow coupling theory. Then, the calculated time-domain responses of the stator and shell vibration velocity of the IWM under different road excitations and the heat sources of each motor component under different speeds are loaded onto the heat flux coupling analysis model of the IWM drive system, and the thermal field characteristics of the IWM drive system under different vibration responses are analyzed. Finally, the influence law of different speeds and road grades on the thermal field characteristics is obtained.

### 3. Determination of heat source of IWM drive system

#### 3.1. Basic structure of the IWM drive system

In this paper, a 15 kW IWM drive system is taken as the research object, the 2-D structure drawing is shown in Fig. 2(a) and the cooling system is shown in Fig. 2(b). The IWM shown in the

figure is a permanent-magnet synchronous motor (PMSM) with an inner rotor and outer stator. The cooling mode is water cooling. The cooling channel structure is of a spiral type. The inlet and outlet are set above the direction of the motor's Z-axis. The main performance parameters of the IWM are shown in Table 1. The basic structural parameters of the water-cooled IWM drive system are shown in Table 2.

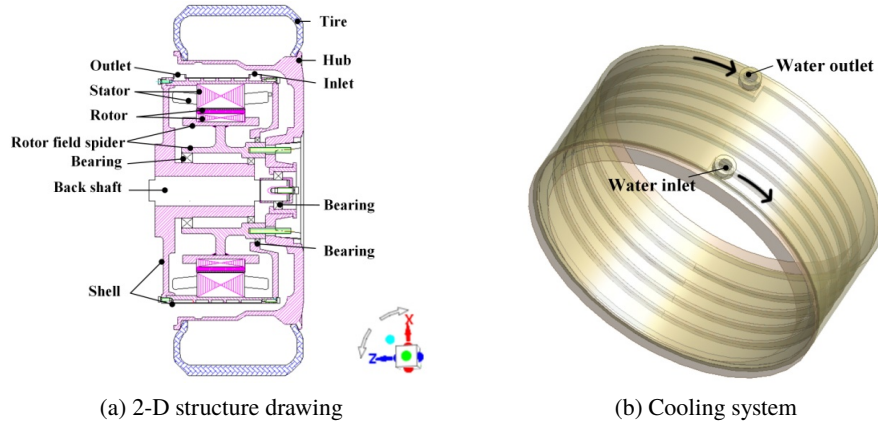


Fig. 2. Structure diagram of the IWM drive system

Table 1. Basic performance parameters of IWM

Name	Value	Name	Value
Rated power	15 kW	Rated speed	1 000 r/min
Rated line voltage	330 V	Phase	3
Rated torque	143 Nm	Winding form	Y

Table 2. Structural parameters of the IWM drive system

Name	Value	Name	Value
Stator outer diameter	310 mm	Number of stator slots	72
Stator inner diameter	240 mm	Number of pole pairs	36
Rotor inner diameter	200 mm	Intake diameter	15 mm
Stator core length	69 mm	Water channel rib thickness	4 mm
Rotor core length	71 mm	Water channel height	10 mm

### 3.2. Determination of heat source

In the running process, the motor will produce more losses, which will eventually be converted into heat, thus posing a threat to the safe operation of the motor. The motor loss mainly includes winding loss, iron core loss, permanent magnet eddy current loss, mechanical loss and stray loss. Due to the small proportion of mechanical loss and stray loss, it is not considered in this paper [14]:

#### 1) Copper loss of winding

The copper loss of the winding of the IWM drive system can be calculated by the formula as follows:

$$P_{cu} = mI^2R, \quad (1)$$

where: the copper loss of windings is represented by  $P_{cu}$ ; the number of motor phases is represented by  $m$ , taking 3; the motor stator current is represented by  $I$ ; the motor stator resistance is represented by  $R$ .

#### 2) Loss of stator and rotor core

The electromagnetic field generated by the IWM drive system alternates between the stator and rotor, which results in the loss of stator and rotor cores. Generally speaking, the loss of stator and rotor cores can be divided into: hysteresis loss, eddy current loss and additional loss, of which the additional loss can be ignored. The core loss can be calculated by the following formula:

$$P_{Fe} = P_c + P_h = K_c \cdot f B_m^\alpha + K_h \cdot B_m^2, \quad (2)$$

where: the iron loss is represented by  $P_{Fe}$ ; the eddy current loss and hysteresis loss are, respectively, represented by  $P_c$ ,  $P_h$ ; the eddy current loss coefficient and hysteresis loss coefficient are, respectively, represented by  $K_c$ ,  $K_h$ ; the magnetic field frequency is represented by  $f$ ; the magnetic density amplitude is represented by  $B_m$ ; and the coefficient obtained by an empirical formula is represented by  $\alpha$ .

#### 3) Eddy current loss of permanent magnet

When the motor is running, the change of the magnetic field density will produce eddy current in the permanent magnet, which will lead to eddy current loss of the permanent magnet. The eddy current loss of the permanent magnet can be calculated by the following formula:

$$P_{\text{eddy}} = \int_V E \cdot J dV = \int_V \frac{J^2}{\sigma} dV = \int_V \rho J^2 dV, \quad (3)$$

where: the eddy current electric field strength is represented by  $E$ ; the eddy current density is represented by  $J$ ; the permanent magnet conductivity is represented by  $\sigma$ ; the permanent magnet resistivity is represented by  $\rho$ , which is assumed to be isotropic in this paper,  $\rho = 1/\sigma$ ; the volume of the permanent magnetism represented by  $V$ .

According to the loss calculation formula, the loss of the IWM drive system is obtained under the condition that the IWM driven vehicle runs at different speeds and uniform speed on the horizontal road, as shown in Table 3, below [15].

In the calculation of a temperature field, a heat generation rate can be used as the heat source load, and the heat generation rate of each component of the motor can be calculated by Formula (4).

$$q = \frac{P_{\text{loss}}}{V}, \quad (4)$$

Table 3. Heat generation rate of IWM at different speeds

Vehicle speed (km/h)	Winding (W/m <sup>3</sup> )	Stator iron core (W/m <sup>3</sup> )	Rotor iron core (W/m <sup>3</sup> )	Permanent magnet (W/m <sup>3</sup> )
18	3.52	143.84	1.03	0.16
36	14.09	144.22	1.25	0.19
72	56.38	144.83	2.23	0.52
108	160.42	145.59	3.80	1.43
124	318.32	145.62	4.74	2.05
136	511.15	153.40	8.46	5.19

where: the heat generation rate is represented by  $q$ , the volume of the heat generation body is represented by  $V$ , the loss of each component of the motor is represented by  $P_{\text{loss}}$ .

According to the data in Table 3 and Formula (4), the heat generation rate of the IWM drive system is obtained, as shown in Table 4, below.

Table 4. Heat generation rate of IWM at different speeds

Vehicle speed (km/h)	Winding (W/m <sup>3</sup> )	Stator iron core (W/m <sup>3</sup> )	Rotor iron core (W/m <sup>3</sup> )	Permanent magnet (W/m <sup>3</sup> )
18	9 030	84 600	515	67
36	36 100	84 800	625	79
72	145 000	85 200	1 120	217
108	411 000	85 600	1 900	596
124	816 000	85 700	2 370	854
136	1 310 000	90 200	4 230	2 160

## 4. Establishment of heat flow coupling model for IWM drive system

### 4.1. Fundamental assumption

In order to improve the calculation efficiency and accurately analyze the thermal field characteristics of the water-cooled IWM under different road excitations, the following assumptions are made in this paper:

1. The stator winding of the IWM is composed of multiple copper wires, and the outer surface is covered with enameled wire. In order to simplify the model, the wires in the slot are considered to be arranged evenly, and the winding is equivalent to two thick coppers and an insulating layer (Fig. 3) [16]. The influence of other parts of the IWM drive system on the heat radiation of the IWM drive system is ignored;

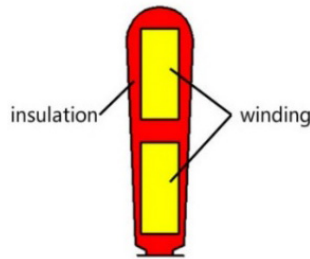


Fig. 3. Equivalent winding

2. The fluid in the cooling structure is incompressible and the flow state is unsteady with time;
3. The radiation effect of other parts of the IWM drive system on the IWM can be ignored;
4. Mechanical losses and stray losses are ignored;
5. Air in the motor cavity is treated as still air except for the air gap.

#### 4.2. Coupling method

The heat dissipation of the water-cooled IWM is a complex process of electromagnetic heat generation, solid heat conduction and fluid heat dissipation. Therefore, the research on the thermal field characteristics of the water-cooled IWM under road excitation involves the interaction of multiple physical fields, such as a vibration field, electromagnetic field, flow field and thermal field. The coupling relationship between the four fields and the coupling factors are marked in Fig. 4, below.

As shown in Fig. 4, the magneto-thermal coupling between the electromagnetic field and the thermal field, the heat-flow coupling between the thermal field and the flow field, and the fluid-structure coupling between the vibration field and the flow field all belong to a strong coupling relationship. According to the analysis in section 2, the influence of the electromagnetic field on the temperature field, the vibration field on the flow field and the flow field on the temperature field are only considered in this paper. Unidirectional coupling is the coupling method adopted in this paper. The unidirectional coupling relationship among the four fields considered in this paper is marked with a red line in the figure, and the influencing factors are represented with red characters.

#### 4.3. Boundary conditions

- 1) The setting of the inlet and outlet boundary conditions

Assuming that all losses of the IWM will be taken away by the coolant, the water inlet flow can be determined by Formula (5):

$$m = \frac{P_{\text{loss}}}{c_p (T_{\text{out}} - T_{\text{in}})}, \quad (5)$$

where: the water inlet flow is represented by  $m$ , kg/s; the total loss of the IWM is represented by  $P_{\text{loss}}$ , W; the specific heat capacity of the coolant is represented by  $c_p$ ; the water outlet

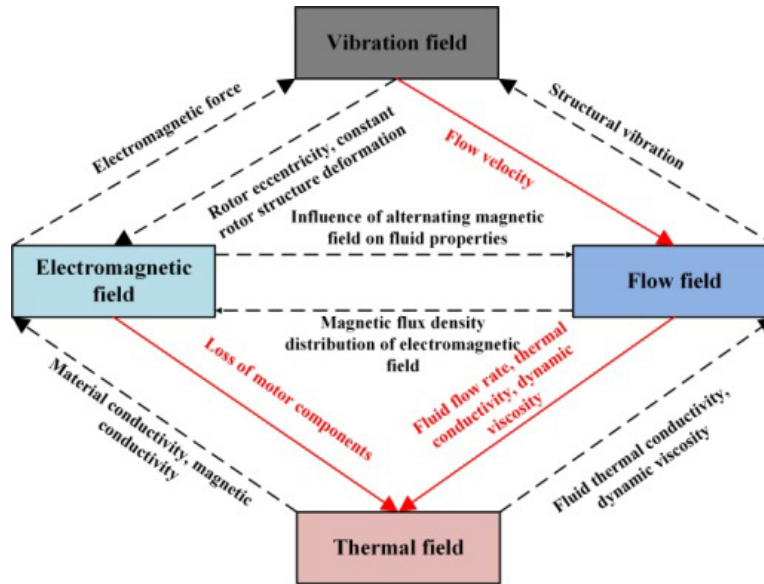


Fig. 4. Diagram of four-field coupling relationship

temperature and the water inlet temperature are, respectively, represented by  $T_{out}$ ,  $T_{in}$  and the temperature difference between the water inlet and the water outlet is set to  $8^{\circ}\text{C}$  in this paper.

The water inlet is set as the velocity inlet, the initial temperature is  $22^{\circ}\text{C}$ , and the water outlet is set as the outflow.

2) The setting of the convective heat transfer coefficient on each surface of the IWM

A large amount of heat is generated by the IWM, which leads to convective heat transfer between the IWM housing and the outside air. The convective heat transfer coefficient on each surface of the IWM can be obtained by the following formula [15]:

$$\alpha = 14 (1 + k\sqrt{v})^3 \sqrt{\frac{\theta}{25}}, \quad (6)$$

where: the coefficient of air flow blowing efficiency is represented by  $k$ , set to  $22^{\circ}\text{C}$  in this paper; the wind speed on the surface of the blowing motor shell is represented by  $v$ ; the room temperature is represented by  $\theta$ , in this paper.

#### 4.4. Thermal conductivity of material

1) Equivalent calculation of air gap thermal conductivity [17, 18]

The heat transfer between the stator and rotor is achieved through the air gap. The air gap is treated as stationary solid in this paper, and the equivalent thermal conductivity ( $\lambda_{eff}$ ) is used to replace the convective heat transfer coefficient.

The Reynolds number in the air gap can be expressed as:

$$\text{Re} = \frac{\omega_{\varphi} l \delta}{\nu}, \quad (7)$$

where:  $\omega_{\varphi 1}$  is the rotor peripheral speed,  $\delta$  is the length of the air gap and  $\nu$  is the kinematic viscosity of the air.

The expression of the critical Reynolds number is:

$$\text{Re}_{cr} = 41.2 \sqrt{\frac{R_i}{\delta}}, \quad (8)$$

where  $R_i$  is the stator inner diameter.

The critical Reynolds number is 475.74.

When  $\text{Re} < \text{Re}_{cr}$ , the air flow in the air gap is laminar, and the effective thermal conductivity  $\lambda_{\text{eff}}$  is equal to the thermal conductivity  $\lambda_{\text{air}}$  of the air. When  $\text{Re} > \text{Re}_{cr}$ , the air flow in the air gap is turbulent. So, the effective thermal conductivity of the air gap can be calculated by the following formula:

$$\lambda_{\text{eff}} = 0.0019\eta^{-2.9084} \cdot \text{Re}^{0.4616 \ln(3.33361\eta)}, \quad (9)$$

where:  $\eta = r_0/R_i$ ,  $r_0$  is the outer diameter of the rotor.

According to the above formula, the equivalent thermal conductivity of the air gap under different working conditions is calculated as shown in Table 5.

Table 5. Equivalent thermal conductivity of air gap under different working conditions

Vehicle speed (km/h)	Thermal conductivity (W/(m·°C))	Vehicle speed (km/h)	Thermal conductivity (W/(m·°C))
18/36/72	0.0267	108	0.0690
124	0.0731	136	0.0771

## 2) Thermal conductivity of other components of the IWM drive system

The materials, thermal conductivity, specific heat capacity and density of each component of the IWM drive system are shown in Table 6.

Table 6. Material attributes of various component of IWM

Name	Material	Density (kg/m <sup>3</sup> )	Thermal conductivity (W/(m·°C))	Specific heat capacity (J/(kg·°C))
Stator and rotor cores	Silicon	7 700	40	426
Winding	Copper	8 900	379	390
Magnet	NdFeB	7 800	6.16	460
Insulation	Insulation	1 300	0.3	1 340
House	45#	7 850	50.2	480

## 5. Calculation results and analysis

The vibration model in this paper adopts the five-degree-of-freedom physical model of the half-car (Fig. 5) established in the previous study of the research group [13].

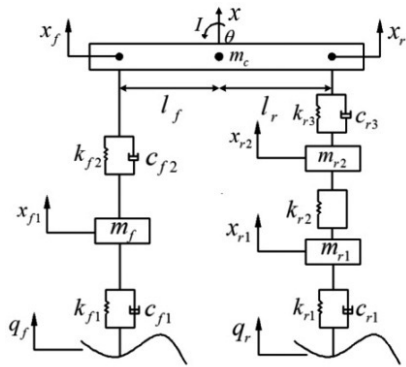


Fig. 5. Velocity response of the IWM stator and shell

The meanings of the symbols in Fig. 5 are as follows:  $m_c$  is the body mass;  $I$  is the body pitching inertia moment;  $m_f$  is the mass of front wheels;  $m_{r1}$  is the total mass of the rear tires, wheel hubs and IWM rotor;  $m_{r2}$  is the total mass of the support shaft, IWM shell and IWM stator;  $l_f$  is the distance from the center of mass to the front axle;  $l_r$  is the distance from the center of the mass to the rear axle;  $\theta$  is the body elevation angle;  $k_{f1}$ ,  $k_{f2}$  are, respectively, the front tire stiffness and front suspension stiffness;  $c_{f1}$ ,  $c_{f2}$  are, respectively, the front tire damping and front suspension damping;  $k_{r1}$ ,  $k_{r2}$ ,  $k_{r3}$  are, respectively, the rear tire stiffness, the bearing stiffness and the rear suspension stiffness;  $c_{r1}$ ,  $c_{r3}$  are, respectively, the rear tire damping and rear suspension damping;  $x_f$ ,  $x_{r1}$ ,  $x_{r2}$  are, respectively, the vertical displacement of corresponding mass block;  $x_f$ ,  $x_r$  are, respectively, the vertical displacement of the vehicle body and suspension connection point;  $q_f$ ,  $q_r$  are the road excitations of the front and rear wheels respectively.

The vibration response characteristics of the IWM stator and shell under different road excitation are obtained through simulation analysis. The time-domain response of the vibration velocity generated by the IWM stator and shell on a B-grade road with a speed of 136 km/h is shown in Fig. 6.

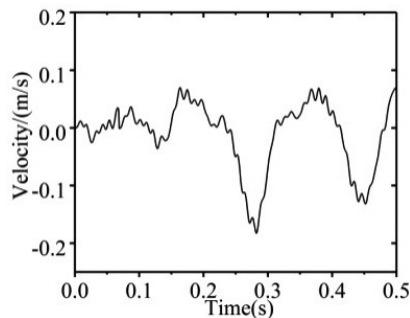


Fig. 6. Velocity response of the IWM stator and shell

### 5.1. Influence of speed on thermal field characteristics of water-cooled IWM

The vibration response of the motor stator and shell and the heat generation rate of each component of the motor on a B-grade road at different speeds are treated as loads in the heat flow coupling analysis model of the IWM drive system. Additionally, the thermal field of the water-cooled IWM at different speeds is calculated. The time-varying curve of temperature of each component of the water-cooled IWM within 0–0.5 s is shown in Fig. 7, below. In the picture, the time-varying curves of the temperature of each component of the water-cooled IWM under road excitation are represented by solid lines, and the time-varying curves of the temperature of each component of the water-cooled IWM without considering road excitation are represented by dashed lines. The time-varying curve of the maximum temperature of each component of the water-cooled IWM is shown in Fig. 7(a), and the time-varying curve of the average temperature of each component of the water-cooled IWM is shown in Fig. 7(b).

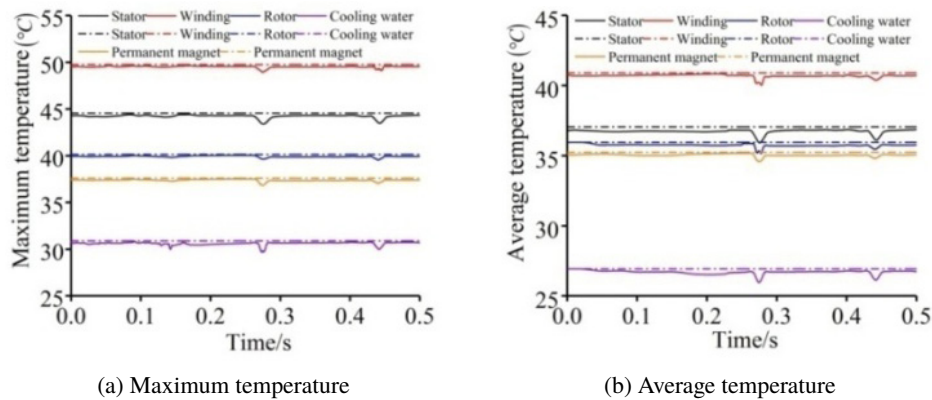


Fig. 7. Time-varying curve of temperature of each component of water-cooled IWM

It can be seen from Fig. 7 that the maximum and average temperatures of each components of the water-cooled IWM remain stable over time within 0–0.5 s without road excitation, and the maximum and average temperatures of each component of the water-cooled IWM fluctuate with time under road excitation. Moreover, under road excitation, the temperature of each component of the water-cooled IWM reaches the lowest at 0.275 s, which is because road excitation has the greatest impact on the IWM cooling system at this time. Among them, the temperature change of the motor stator and winding is most obviously affected by road excitation, and the temperature fluctuation is the largest. This is because the cooling system is excited by road excitation, resulting in a drastic change in the flow field velocity, and the motor stator is closest to the cooling system, so the temperature is most affected by the flow field characteristics.

The thermal field characteristics of the IWM drive system at speeds of 18 km/h, 36 km/h, 72 km/h, 108 km/h, 124 km/h and 136 km/h are simulated and analyzed based on road excitation and without considering road excitation. The variation curves of the root mean square (RMS) value of the average temperature of each component of the motor at different speeds from 0 to 0.5 s are shown in Fig. 8. In the picture, the average temperature of each component of the IWM

under road excitation is represented by solid lines, and the average temperature of each component of the IWM without considering road excitation is represented by dashed lines.

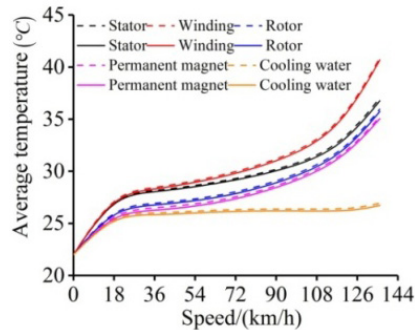


Fig. 8. Average temperature of each component of the IWM

It can be seen from Fig. 8 that the average temperatures of various components of the IWM increase with the increase of vehicle speed. This is because as the driving speed of IWM driven vehicles increases, higher power needs to be provided by the IWM to achieve the required speed of the vehicle, which will increase the loss of the IWM during operation and lead to the increase of the temperature of each component of the IWM. Additionally, the average temperature of each component of the IWM is obviously lower when it is stimulated by the road than when it is not stimulated by the road. At a vehicle speed of 136 km/h, the temperature of the motor stator, winding, rotor and permanent magnet under road excitation decreases by 0.76%, 0.54%, 0.60% and 0.58%, respectively.

## 5.2. Influence of road grade on thermal field characteristics of water-cooled IWM

As the input of vehicle vibration, the statistical characteristics of road roughness are mainly described by road power density. Reference [19] proposed that the unevenness of the road can be divided into 8 levels according to the road power spectral density. With the increase of road power spectral density, the road grade increases gradually. This will cause the vehicle to vibrate more violently.

In order to analyze the thermal field characteristics of the IWM drive system more accurately at different road grades, the thermal field characteristics of the IWM drive system under the excitation of A-grade, C-grade and D-grade roads are analyzed respectively, when the IWM driven vehicle at a speed of 136 km/h reaches a stable state. The time-varying curve of temperature of each component of the water-cooled IWM within 0–0.5 s is shown in Fig. 9 below. In the picture, the time-varying curves of the temperature of each component of the water-cooled IWM under road excitation are represented by solid lines, and the time-varying curves of the temperature of each component of the water-cooled IWM without considering road excitation are represented by dashed line. The time-varying curve of the maximum temperature of each component of the water-cooled IWM is shown in Fig. 9(a), and the time-varying curve of the average temperature of each component of the water-cooled IWM is shown in Fig. 9(b).

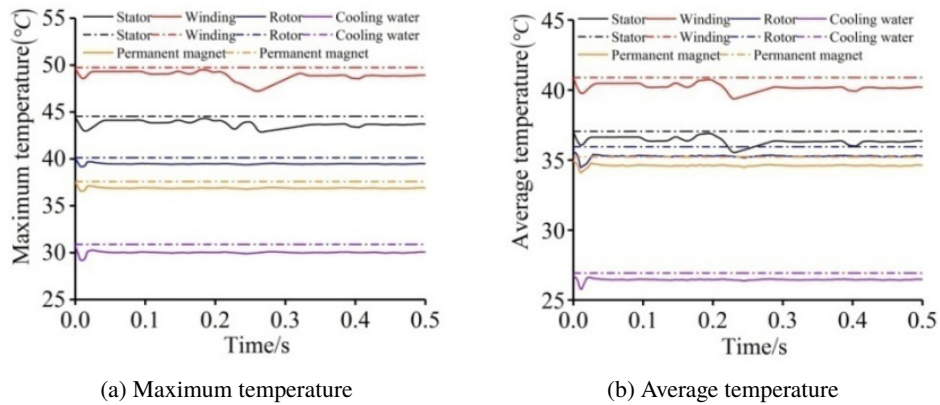


Fig. 9. Time-varying curve of temperature of each component of water-cooled IWM

It can be seen from Fig. 9 that the maximum and average temperatures of each components of the water-cooled IWM remain stable over time within 0–0.5 s without road excitation. The maximum and average temperatures of each component of the water-cooled IWM under road excitation change constantly with time. In this figure, the components with more obvious changes are the motor stator and windings, because the motor stator and windings are most affected by the convective heat transfer of coolant. As the cooling water flows along the Z-axis spiral in the cooling system, the heat generated by each part of the IWM is constantly taken away, resulting in a relatively gentle temperature change of the coolant.

Based on the above simulation analysis, the thermal field characteristics of the water-cooled IWM under different road roughness coefficients are analyzed. The root mean square (RMS) of the average temperature of each component of the water-cooled IWM within 0–0.5 s was calculated under different road roughness coefficients, as shown in Fig. 10.

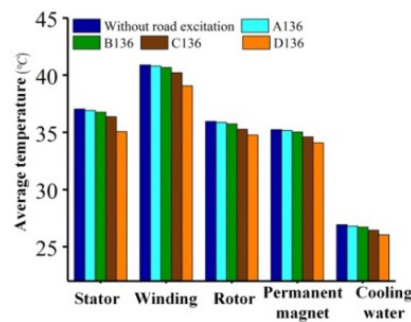


Fig. 10. Average temperature of each component of the water-cooled IWM

It can be seen from Fig. 10 that the average temperatures of various components of the IWM decrease with the increase of road roughness coefficients. Among them, the temperature variation of the motor stator is most obviously affected by road excitation, and the temperature fluctuation

is the largest. This is the closest distance between the motor stator and the cooling system, and the temperature is greatly affected by the flow field characteristics. Under the vibration action of A-grade, B-grade, C-grade and D-grade road excitation: the average temperature of motor stator decreased by 0.34%, 0.76%, 1.80% and 5.32%, respectively; the average temperature of the motor winding decreased by 0.22%, 0.54%, 1.68% and 4.48%, respectively; the average temperature of the motor rotor decreased by 0.21%, 0.60%, 1.90% and 3.28%, respectively; and the average temperature of the motor permanent magnets decreased by 0.23%, 0.58%, 1.80% and 3.30%, respectively.

## 6. Conclusions

The driving system of the water-cooled IWM is taken as the research object in this paper. The heat flow coupling method is adopted. On the basis of calculating the excitation load and the heat source load of each component, the thermal field characteristics of the water-cooled IWM under road excitation are numerically simulated by using the method of heat flow coupling. In addition, the influence of road excitation on the thermal field characteristics of each component of the water-cooled IWM is analyzed. The following conclusions are obtained:

1. The IWM is installed on wheels, and road excitation acts on the IWM directly through a wheel. This affects the flow field characteristics of the IWM cooling system, and affects the heat dissipation of the IWM and the distribution of the thermal field of each component.
2. The thermal field characteristics of the water-cooled IWM are affected by the speed of the IWM-driven vehicle and road grades. At the same road grade, the temperature reduction amplitude of each component of the water-cooled IWM increases nonlinearly with the increase of vehicle speed. At a vehicle speed of 136 km/h, the temperature of a motor stator, winding, rotor and permanent magnet under road excitation decreases by 0.76%, 0.54%, 0.60% and 0.58%, respectively. At the same speed, the average temperature of each component of the water-cooled IWM decreases with the increase of road roughness. The road grades goes from A to D, and the temperature of the motor stator, winding, rotor, permanent magnet and coolant drops by 5.0%, 4.3%, 3.1%, 3.1% and 2.9%, respectively. From the comparative analysis of simulation data, it can be seen that road grades have a greater impact on thermal field characteristics of the water-cooled IWM. However, the thermal field distribution of local parts of motors is relatively uneven under road excitation, which leads to greater thermal stress of the local parts and increase the risk of motor damage.
3. In order to further determine the accuracy of the results, it is necessary to build an experimental bench of the water-cooled IWM under road excitation to simulate the real environment of vehicle operation and further verify its correctness.

## Acknowledgements

This research is supported by the National Nature Science Foundation of China (Grant no. 51775320) and sponsored by Shandong Province Key Research and Development Program (Grant no. 2019GGX104069).

## References

- [1] Chen Yi, Yao Yihua, Lu Qinfen, Huang Xiaoyan, Ye Yunyue, *Thermal modeling and analysis of double-sided water-cooled permanent magnet linear synchronous machines*, COMPEL-The International Journal for Computation and Mathematics in Electrical and Electronic Engineering, vol. 35, no. 2, pp. 695–712 (2016).
- [2] Qiu Hongbo, Zhang Yong, Yang Cunxiang, Yi Ran, *Performance analysis and comparison of PMSM with concentrated winding and distributed winding*, Archives of Electrical Engineering, vol. 69, no. 2, pp. 303–317 (2020).
- [3] Kim S.C., Kim W., Kim M.S., *Cooling performance of 25 kW in-wheel motor for electric vehicles*, International Journal of Automotive Technology, vol. 14, no. 4, pp. 559–567 (2013).
- [4] Karnavas Y.L., Chasiotis I.D., Peponakis E.L., *Cooling system design and thermal analysis of an electric vehicle's in-wheel PMSM*, Proceedings of the 2016 XXII International Conference on Electrical Machines (ICEM), Lausanne, Switzerland, pp. 1439–1445 (2016).
- [5] Ding Yonggen, Xu Tianji, Zhang Nan, Hai Lu, *Analysis of Drive Motor Housing Cooling Structure Design and Thermal Simulation of New Energy Vehicle*, Auto Time, vol. 16, pp. 71–72 (2020).
- [6] Zhao Lanping, Jiang Congxi, Xu Xin, Yang Zhigang, *The Effects of Oil Cooling on the Temperature Field of Out-rotor In-wheel Motor Under Vehicle Operation Environment*, Automotive Engineering, vol. 41, no. 4, pp. 373–380 (2019).
- [7] Gao Panpan, *Study on Cooling and Heat Transfer about Electrical Transmission System of Wheeled Vehicle*, Master Thesis, Department of Mechanical Engineering, Beijing Institute of Technology, Beijing (2015).
- [8] Funieru B., Binder A., *Thermal design of a permanent magnet motor used for gearless railway traction*, Proceedings of the 2008 34th Annual Conference of the IEEE Industrial Electronics Society, Orlando, FL, USA, pp. 2061–2066 (2008).
- [9] Chien C.H., Jang J.Y., *3-D numerical and experimental analysis of a built-in motorized high-speed spindle with helical water cooling channel*, Applied Thermal Engineering, vol. 28, no. 17–18, pp. 2327–2336 (2008).
- [10] Zeng Jinling, Xu Yu, Han Yepeng, Li Guanhua, Zhang Qun, *Cooling Simulation Analysis Based on Multi-Field Coupling Technology of Permanent Magnet Synchronous Motor*, Journal of Shanghai Jiaotong University, vol. 48, no. 9, pp. 1246–1251+1256 (2014).
- [11] Huang Z., Marquez F., Alakula M., Yuan J., *Characterization and application of forced cooling channels for traction motors in HEVs*, Proceedings of the 2012 XXth International Conference on Electrical Machines, Marseille, France, pp. 1212–1218 (2012).
- [12] Zheng Ping, Liu R., Thelin P., Nordlund E., Sadarangani C., *Research on the Cooling System of a 4QT Prototype Machine Used for HEV*, IEEE Transactions on Energy Conversion, vol. 23, no. 1, pp. 61–67 (2008).
- [13] Tan Di, Wang Qiang, *Modeling and Simulation of the Vibration Characteristics of the In-Wheel Motor Driving Vehicle Based on Bond Graph*, Shock and Vibration, vol. 1, pp. 1–14 (2016).
- [14] Li Donghe, *Analysis on Temperature Field of Oil-Cooled Motor Used in Vehicles*, Small and Special Electrical Machines, vol. 44, no. 7, pp. 37–40 (2016).
- [15] Song Fan, *Research on heating and cooling of in-wheel motor drive system*, Master Thesis, Department of Transportation and Vehicle Engineering, Shandong University of Technology, Zibo (2019).
- [16] Weili Li, Shoufa Li, Ying Xie, *Stator-rotor Coupled Thermal Field Numerical Calculation of Induction Motors and Correlated Factors Sensitivity Analysis*, Proceedings of the CSEE, vol. 24, pp. 85–91 (2007).

- 
- [17] Chai F., Tang Y., Pei Y. *et al.*, *Temperature Field Accurate Modeling and Cooling Performance Evaluation of Direct-Drive Outer-Rotor Air-Cooling In-Wheel Motor*, *Energies*, vol. 10, no. 9, p. 818 (2016).
- [18] Lei Liu, *The Study of Thermal Characteristics in Various Conditions and Cooling System of Permanent Magnet Synchronous Motor in Pure Electric Vehicle*, Hefei University of Technology, Master Thesis (2015).
- [19] Lin Maocheng, Zhao Jihai, *GB 7031-1987 Vehicle vibration input - pavement flatness representation method*, Standard Press of China (1987).